Univerzita Komenského v Bratislave

Fakulta matematiky, fyziky a informatiky

Ing. Prerna Chauhan

Autoreferát dizertačnej práce

III-N quantum structures for new generation of ultra-fast transistors

na získanie akademického titulu philosophiae doctor

v odbore doktorandského štúdia:

Fyzika kondenzovaných látok a akustika

Bratislava 2019

Dizertačná práca bola vypracovaná v dennej forme doktorandského štúdia na Elektrotechnický ústav Slovenskej akadémie vied (SAV) v Bratislava

Predkladateľ: Ing. Prerna Chauhan
Elektrotechnický ústav SAV
Dúbravská cesta 9
841 04 Bratislava

Školiteľ: Ing. Ján Kuzmík, DrSc.
Elektrotechnický ústav SAV
Dúbravská cesta 9
841 04 Bratislava

študijný odbor: Fyzika kondenzovaných látok a akustika

Predseda odborovej komisie:

Prof. RNDr. Peter Kúš, DrSc.
FMFI UK
Mlynská dolina
842 48 Bratislava

Abstract

Gallium nitride (GaN) based semiconductors or group III-nitrides, aluminum nitride (AlN), GaN, indium nitride (InN) and their alloys, are universal materials and have got applications in variety of electronic and optoelectronic devices due to their distinctive properties and gravity for electronics and optoelectronics, respectively. GaN based devices have revolutionized over the past decades and nowadays, replacing the Si and other III-V semiconductors based devices. Utmost of $Al_xGa_{1-x}N$/GaN technologies are now well known and to vanquish them, alternative technologies are assiduously investigated by research societies. Out of group III-nitrides and other well know semiconductors, InN has the lowest effective electron mass, and consequently has higher mobility and highest saturation electron drift velocity. This excellently electron transport property of InN establishes it as the best candidate for channel in high electron mobility transistors (HEMTs). However, due to the InN growth issues, InN based devices are still at an early stage. But, it is certain that InN is a promising new material for future devices. Growth of indium (In)-rich $In_xAl_{1-x}N$ ternary alloy as a buffer layer can be very useful in providing less compressive strain to InN channel.

The goal and prime focus of the thesis are on: i) to grow In-rich $In_xAl_{1-x}N$ semi-insulating buffer layer by OMCVD; ii) preparation of InAlN/InN quantum well, iii) investigate the structural, surface, compositional, electrical and optical properties of layers by various characterization tools; iv) studying the influence of change in growth parameters on layers properties.

To increase the indium composition in $In_xAl_{1-x}N$ layer, three growth parameters are optimized. First optimized parameter is growth temperature while keeping others constant. After that, the impact of growth pressure and ammonia flow on indium composition and layer properties are investigated. Phase separation and gallium auto-incorporation being the mostly known growth issues of $In_xAl_{1-x}N$, are also investigated. The growth of $In_xAl_{1-x}N$ buffer layer directly on c-sapphire is proved a milestone for this work and we achieved high quality In-rich $In_{0.60}Al_{0.40}N$ layer. Subsequently, growth of InN channel layer is reported on In-rich $In_xAl_{1-x}N$ buffer layer.

Keywords: OMCVD; $In_xAl_{1-x}N$; InN; structural, optical, chemical and electrical characterization.

Abstrakt

Polovodiče na báze nitridu gália (GaN) alebo nitridy skupiny III, nitrid hliníka (AlN), GaN, nitrid india (InN) a ich zliatiny, sú univerzálnymi materiálmi a vďaka svojim charakteristickým vlastnostiam majú uplatnenie v rôznych elektronických a optoelektronických zariadeniach pre elektroniku a optoelektroniku. Zariadenia založené na GaN sa v posledných desaťročiach revolucionizovali a nahradili polovodiče na báze Si a ďalších III-V. Väčšina technológií $\mathrm{Al}_x\mathrm{Ga}_{1-x}\mathrm{N}$/ GaN je dnes dobre známa a na ich prekonanie sú alternatívne technológie neúnavne skúmané výskumnými spoločnosťami. Z nitridov III. skupiny a ďalších dobre známych polovodičov má InN najnižšiu efektívnu hmotnosť elektrónov, a teda má vyššiu mobilitu a najvyššiu rýchlosť elektrónov. Táto vynikajúca vlastnosť elektrónového transportu v InN ho robí najlepším kandidátom na kanál v tranzistoroch s vysokou pohyblivosťou elektrónov (HEMT). Z dôvodu problémov s rastom InN sú však súčiastky založené na InN stále v počiatočnom štádiu vývoja. Je však isté, že InN je sľubným novým materiálom pre budúce zariadenia. Rast $\mathrm{In}_x\mathrm{Al}_{1-x}\mathrm{N}$ nárazníkovej vrstvy s vysokým obsahom In môže byť veľmi užitočný pri poskytovaní menšieho kompresného napätia v InN kanáli.

Cieľom a hlavným zameraním práce je: i) študovať $\mathrm{In}_x\mathrm{Al}_{1-x}\mathrm{N}$ poloizolačnú nárazníkovú vrstvu pomocou OMCVD; ii) pripraviť $\mathrm{In}_x\mathrm{Al}_{1-x}\mathrm{N}$/InN kvantovú jamu, iii) skúmať štrukturálne, povrchové, kompozitné, elektrický a optické vlastnosti vrstiev pomocou rôznych charakterizačných nástrojov; iv) štúdium vplyvu zmeny rastových parametrov na vlastnosti vrstiev

Na zvýšenie zloženia india vo vrstve $\mathrm{In}_x\mathrm{Al}_{1-x}\mathrm{N}$ sa optimalizujú tri rastové parametre. Prvým optimalizovaným parametrom je teplota rastu, zatiaľ čo ostatné sú konštantné. Potom sa skúma vplyv rastového tlaku a toku amoniaku na obsah india a vlastnosti vrstvy. Preskúmala sa tiež separácia fáz a autointegrácia gália, ktoré sú väčšinou známymi problémami rastu $\mathrm{In}_x\mathrm{Al}_{1-x}\mathrm{N}$. Rast vrstvy $\mathrm{In}_x\mathrm{Al}_{1-x}\mathrm{N}$ priamo na c-zafíri sa ukázal ako míľnik pre túto prácu a dosiahli sme vysoko kvalitnú vrstvu $\mathrm{In}_{0.60}\mathrm{Al}_{0.40}\mathrm{N}$ s vysokým obsahom india. Následne sa na nárazníkovej vrstve $\mathrm{In}_x\mathrm{Al}_{1-x}\mathrm{N}$ pripravil a testoval rast InN kanála.

Kľúčové slová: OMCVD; $\mathrm{In}_x\mathrm{Al}_{1-x}\mathrm{N}$; InN; štrukturálne, povrchové, kompozitné, elektrický a optické charakterizačných.

Table of Contents

1 Introduction **1**

2 State of the knowledge of InN based semiconductors **2**

2.1 Advantages of InN-channel in HEMTs……………………………………….......2

2.2 Metalorganic Chemical Vapor Deposition System (MOCVD)……………........3

2.3 Growth issues of InN……………………………………………………….......3

2.4 Growth issues of In-rich InAlN Buffer layer……………………..................4

3 Results **6**

3.1 Growth of In-rich InAlN buffer layers……………………………………….....6

3.1.1 Effect of growth temperature and carrier gas on InAlN…………………6

3.1.2 Effect of pressure and Ammonia flow on InAlN…………………………8

3.1.3 Effect of strain on In-incorporation in InAlN layers……………………10

3.2 Growth and properties of InN/InAlN heterostructures………………………..12

Summary **14**

List of publications **14**

References **16**

1. Introduction

In a recent time, the research interest has been expanded into the usage of terahertz (THz) electromagnetic waves for ultra-high speed circuits integrated in Information and Communication Technology (ICT) systems, which include THz imaging systems, wireless communication and spectroscopy detection. At the present time, semiconductor inter-sub-band sources, such as quantum cascade lasers (QCLs) are being developed as THz emitters, and for THz detection, Schottky diode with integrated oscillator can possibly be used. Mechanism of these optical devices rely on the electron-phonon interaction, and up till now THz QCLs work only at low temperatures, which make them impractical for applications. New proposition for the THz devices that rest absolutely on high power electronics is thus challenging as well as transformative.

This dissertation thesis reports the growth of In-rich InAlN epitaxial layer, which further will be used as a buffer layer for InN channel layer to reduce the compressive strain. InN is very auspicious semiconductor for future generation high frequency electronics. In spite of the remarkable prospective of InN (as mentioned in Table I), reports on InN channel HEMTs are limited only up to theoretical proposals[1] and numerical simulation[2], but due to the InN growth issues, there is no experimental report on such devices till now.

Table I: Glimpse of physical and electron transport parameters of group III-nitrides along with other most popular semiconductors, at room temperature (RT).[3]

Properties	Si	GaAs	SiC	GaN	AlN	InN
Energy Bandgap E_g ((eV)	1.12	1.43	3.26	3.4	6.2	0.7
Maximum Breakdown Field E_b ((MV/cm)	0.3	0.4	3	7.6	51.88	0.1
Electron effective mass m_{eff} (m_o)	0.26	0.068	0.42	0.20	0.40	0.042
Electron Mobility μ_n (cm^2/Vs)	1500	8500	1000	1250	300	4000
Saturation electron drift Velocity υ_{sat} (10^7cm/s)	1	0.72	2	1.9	< 1	1.4
Peak electron drift velocity υ_{peak} (10^7cm/s)	1	2	-	2.9	~1	6.0
Thermal conductivity λ (W/cm K)	1.5	0.5	4.9	2.3	2.85	0.45

2. State of knowledge of InN based semiconductors

2.1. Advantages of InN-channel in HEMTs

The speed of the devices like Field Effect Transistors (FETs), depends on the electron velocity in the channel. In these devices, the channel is heavily doped which limits the mobility by extrinsic carrier scattering. To circumvent this limitation and to achieve high electron mobility, i.e. electrons free from scattering effects, one technique is to use High Electron Mobility transistors (HEMTs). Other names of HEMT are Modulation-doped FET (MODFET) and Two-Dimensional Electron Gas FET (TEGFET). The current gain cut-off frequency (f_T) of HEMTs is coupled with electron transit time (τ) in 2DEG across the gate by the following relation:

$$f_T = {}^{1}\!/_{2\pi\,\tau} = {}^{1}\!/_{2\pi\,\tau_i + \tau_D + \tau_{RC}} \quad (2.1)$$

where intrinsic carrier transit time $\tau_i = L_g/\langle v_e \rangle$, L_g is gate length and $\langle v_e \rangle$ is effective electron velocity, τ_D is parasitic extension of gate region, and τ_{RC} is RC related parasitic delay. Now, it can be realize that faster the electrons transit under the gate, higher will be the f_T. By reducing the L_g, and increasing the electric field across the gate or choosing a semiconductor of highest drift velocity as a channel, the highest possible value of f_T will be

$$f_{T,max} = {}^{v_{max}}\!/_{2\pi L_g} \quad (2.2)$$

InN with the smallest energy band gap, and consequently the lowest effective electron mass and the highest peak velocity (as mentioned in Table I) is really very promising as channel for III-N HEMT technology development in the direction of Terahertz frequency range applications. Strained InN channel on relaxed (0.1-1 μm) $In_{0.9}Al_{0.1}N$ for normally-on and off HEMTs has been proposed by Kuzmík et al.[1] High In mole fraction $In_xAl_{1-x}N$ buffer layer on GaN provides less compressive strain to the strained InN channel (<10 nm), and consequently, replacement of conventional GaN buffer layer by relaxed In-rich $In_xAl_{1-x}N$ buffer layer has been suggested. If GaN channel is replaced by InN in III-N HEMTs, subsequently f_T will increase by a factor of ~2.5 along with ballistic electron transport[3] and THz frequency range should be conveniently accessible.

2.2. Metalorganic Chemical Vapor Deposition System (MOCVD)

The metal–organic chemical vapor deposition (MOCVD) process, also called organometallic chemical vapor deposition (OMCVD), metalorganic vapor phase epitaxy (MOVPE), organometallic vapor phase epitaxy (OMVPE). Materials having low vapor pressure are difficult to transport in the gas form for growth. One solution is to attach organic compound (Methyl, Ethyl etc.) to the low vapor pressure material (Ga, In, Al etc.), because organic compounds have very high vapor pressure. The common metalorganic (MO) precursors for group–III elements (Ga, In, Al etc.) are Trimethylgallium (TMG, $Ga(CH_3)_3$), Trimethylindium (TMIn), and Trimethylaluminum (TMAl or TMA) etc. and for group N elements are ammonia (NH_3). Depending on III-N semiconductor, inert gas like, hydrogen (H_2) or nitrogen (N_2) or their mixture ($H_2 + N_2$) is used as carrier gas to transport precursors up to the substrate.

2.3. Growth issues of InN

Among the group III-N semiconductors, InN is the most difficult to be grown by MOCVD. Growth of InN is still in an immature stage and preventing its usage in THz electronics. The cation (In)-anion (N) binding energy of InN (1.93 eV) is much weaker than the corresponding binding energy of AlN (2.88 eV) and GaN (2.2 eV). Consequently, InN has lower dissociation temperature (≤ 600 ºC) in comparison to AlN and GaN.[4]

In MOCVD, for the InN growth following chemical reaction is used which involves pyrolysis of TMIn and NH_3 on heated substrate which are carried by N_2 carrier gas:

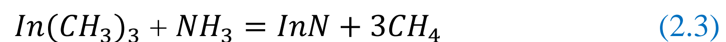

$$In(CH_3)_3 + NH_3 = InN + 3CH_4 \qquad (2.3)$$

To grow InN, growth temperature must be lower than the InN dissociation temperature and this requirement makes the InN growth very difficult by MOCVD due to the low growth rate, caused by the low pyrolysis rate of NH_3 at the low growth temperature of InN.

Figure 2.1(a) illustrate that at low temperature In droplets dominate, while at higher etching mode becomes dominant. This indicate that high input NH_3 pressure

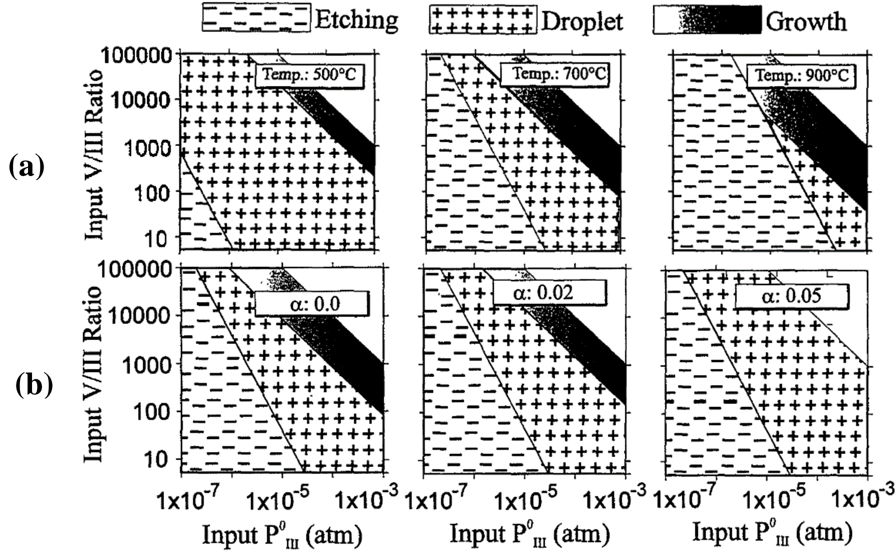

Figure 2.1: Calculated phase diagrams of InN at (a) 500 °C, 700 °C and 900 °C for input partial pressure of group III metal organic species P_{III}^{0} (= P_{In}^{0}) versus input V/III ratio. Etching, In droplets and film growth are three deposition modes. (b) Three mole fractions of decomposed NH_3, α = 0.0, 0.02, and 0.05 for P_{III}^{0} (= P_{In}^{0}) versus input V/III ratio. Etching, In droplets and film growth are three deposition modes.[5]

(= P_{In}^{0} x V/III ratio) is required to grow InN without etching or droplet. With the increasing mole fraction of decomposed NH_3 (α) InN growth area decreases drastically. This is attributed to the fact that increased partial pressure of decomposed NH_3 drives the equation (2.3) to the left. Therefore, growth conditions and reactor design must prevent NH_3 decomposition before reaching the substrate and N_2 is favorable as a carrier gas because H_2 plays very sensitive role in the InN based semiconductors.

MOCVD is well established for industrial production with high yield, however, InN growth is indeed very challenging.

2.4. Growth issues of In-rich InAlN Buffer layer

To grow InN, there is no lattice matched substrate. To solve this lattice mismatch issue between InN and substrate, like sapphire, GaN will be used as first buffer layer due to its more matured growth technology, which is followed by the In-rich $\mathrm{In}_x\mathrm{Al}_{1-x}\mathrm{N}$ second buffer layer to provide less compressive strain to InN channel. Growth of the In-rich buffer layer is the second most important target in the development of InN channel transistor technology.

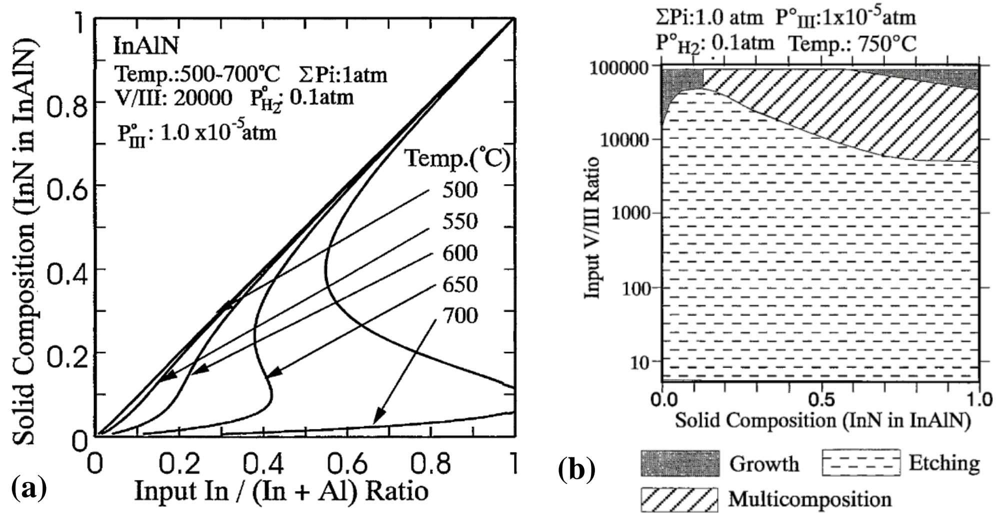

Figure 2.2: (a) In the temperature range of 500 °C to 700 °C, theoretical curves demonstrating In composition variation in InAlN as a function of input mole ratio of MO sources TMIn/(TMIn + TMAl), and (b) Calculated phase diagrams of InAlN at 750 °C, presenting deposition modes as function of the In composition in InAlN and the input V/III ratio.[6]

Figure 2.2(a) shows theoretical curves demonstrating the influence of growth temperatures on the variation of In composition as a function of input MO mole ratio. The important feature worth mentioning in this figure is that the change in iso-temperature lines is more sensitive and complex at higher growth temperatures. This points out that for a given input TMIn/(TMIn + TMAl) ratio, unstable regions with various In compositions is expected in this $In_{x}Al_{1-x}N$ ternary alloy system, which increases with increasing temperature.

Calculated phase diagrams of $In_{x}Al_{1-x}N$ at 750 °C, presenting deposition modes as function of the In composition in $In_{x}Al_{1-x}N$ and the input V/III ratio is shown in Figure 2.2(b). Region with several compositions or unstable multicompositional region exists just above the etching region and growth region small. At low temperature, unstable region materializes at low V/III ratio, which shifted to higher V/III ratio with increasing growth temperature. Consequently, it is obligatory to use high V/III ratio at high growth temperature to achieve good quality $In_{x}Al_{1-x}N$. Complicated variation of the compositional distribution as depicted in Figure 2.2(a) is due to the solid phase issues of $In_{x}Al_{1-x}N$ ternary alloy, which is the inception of the formation of the unstable region. Thermodynamic analysis of Koukitu et al.[6] has illustrated the difficulties in the growth of ternary $In_{x}Al_{1-x}N$ alloy that increases with the increasing In composition.

3. Results

3.1. Growth of In-rich InAlN buffer layers

3.1.1. Effect of growth temperature and carrier gas on InAlN

Table II: Growth parameters for $In_xAl_{1-x}N$ layers along with their *x* values, 0002 and $10\bar{1}1$ ω scan FWHM, and calculated in-plane $10\bar{1}0$ mosaic FWHM, ρ_s and ρ_e. Two values of '*x*' come from 2 peaks in diffraction scan.

T_{growth} (°C)	Carrier gas	$In_xAl_{1-x}N$ *x*	0002		$10\bar{1}1$	$10\bar{1}0$		$r = \rho_e/\rho_s$
			FWHM (°)	ρ_s (10^9 cm^{-2})	FWHM (°)	FWHM (°)	ρ_e (10^{10} cm^{-2})	
790	H_2 (2.4 %)	0.12 / 0.09	0.20	2.1	0.60	0.67	6.2	29
775	H_2 (2.4 %)	0.13 / 0.11	0.22	2.6	0.62	0.69	6.6	26
760	H_2 (2.4 %)	0.15	0.17	1.5	0.32	0.35	1.7	11
730	H_2 (2.4 %)	0.18	0.12	0.8	0.40	0.45	2.8	36
730	N_2 (100 %)	0.37	0.66	23.3	1.6	1.78	43.8	19

A series of $In_xAl_{1-x}N$ layers are grown on GaN buffer layer in sequence (without breaking the growth after GaN). Consequently, unintentional Ga auto incorporation due to memory effect of GaN buffer is going to be the obvious problem here, according to previous reports.[7] Due to this Ga incorporation in InAlN, intended $In_xAl_{1-x}N$ ternary alloy becomes $In_xAl_yGa_{1-x-y}N$ quaternary alloy. Different growth conditions for $In_xAl_{1-x}N$ are shown in Table II. Under H_2 carrier gas, In-incorporation, growth rate (R_g), and surface roughness increases with decreasing $In_xAl_{1-x}N$ growth temperature. Variation in sheet carrier concentration (n_s) with

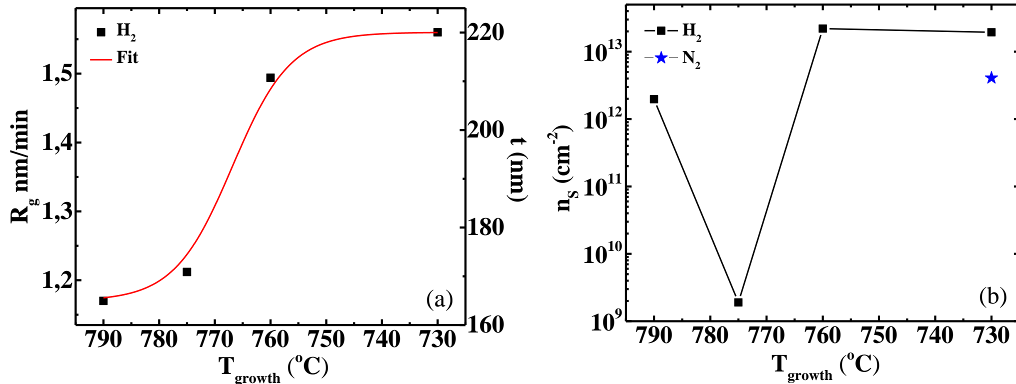

Figure 3.1. (a) Growth rate, R_g, and corresponding thickness, *t*, and (b) n_s vs growth temperature, T_g.

growth temperature (T_g) and carrier gas is demonstrated in Figure 3.1(b). We suggest that presence of H_2 and decreasing T_g, could decrease NH_3 decomposition rate and subsequently, N vacancies (V_N) or donor extra free electrons will increase. Good In-molar fraction homogeneity of $In_xAl_{1-x}N$ layers grown at 760 (x=0.15) and 730 °C (x=0.18) with H_2 carrier gas could provide better 2DEG confinement at $In_xAl_{1-x}N$/GaN interface, which is verified by the Hall, and for both samples n_s ($\sim 2 \times 10^{13}$ cm^{-2}) is nearly same as polarization charge.[8] Though, with N_2 carrier gas at 730 °C, one order lower n_s ($\sim 4 \times 10^{12}$ cm^{-2}) of $In_{0.37}Al_{0.63}N$ layer could be attributed to the lower concentration of V_N and higher ρ_e than $In_{0.18}Al_{0.82}N$ layer grown with H_2 carrier gas; and also due to the eliminated polarization charge at $In_xAl_{1-x}N$/GaN interface for x~0.37.[8]

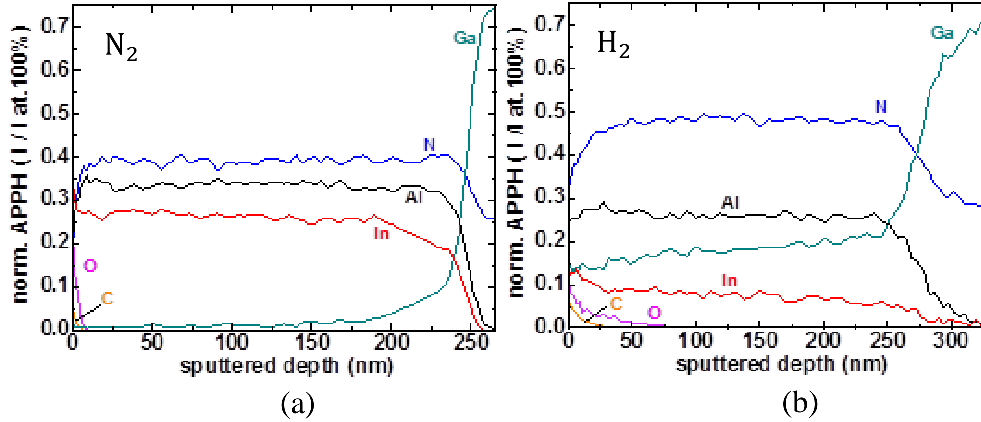

Figure 3.2. Auger depth profile of $In_xAl_{1-x}N$ layer (a) N_2 (100 %), (b) H_2 (2.4 %) grown at 737 °C. Showing the quasi-concentration. This is concertation, but with the relative sensitivity factors equal to 1 for all elements, which is also called normalised auger-peak-to-peak-height (norm. APPH).

In Figure 3.2(a) observed In profile in $In_xAl_{1-x}N$ grown with N_2 carrier gas is quite stable for top 175 nm along with indistinguishable Ga, however for around 100 nm thickness after GaN buffer growth quaternary alloy $In_xAl_yGa_{1-x-y}N$ formation with decreasing Ga concentration towards surface is possible. As expected, H_2 makes In incorporation harder into the $In_xAl_{1-x}N$ layer in Figure 3.2(b).

We are reporting lower n_s than other previous reports, and variation in n_s is inversely proportional to ρ_e. Ga-auto-incorporation provides very useful compositional grading to grow smooth and thick $In_{0.37}Al_{0.63}N$ layer under 100% N_2 carrier gas ambient. Use of N_2 carrier gas increases ρ_e and In-incorporation; reduces

RMS surface roughness 10 times and n_s by an order of magnitude. Edge TDs at grain boundaries are traps, and create negatively charged deep acceptors energy level in forbidden energy bandgap of $In_{0.37}Al_{0.63}N$. The present work points out that unintentional Ga-auto-incorporation in $In_xAl_{1-x}N$ during OMVPE growth under N_2 carrier gas ambient could be an attractive solution to grow thick resistive $In_xAl_{1-x}N$ buffer layer. Moreover, it is suggested that under N_2 carrier gas ambient decreasing Ga-auto-incorporation in $In_xAl_{1-x}N$ layer with growth progression, which create un-intentional compositionally graded layer, could pave the way towards the growth of resistive buffer layer for the InN-channel HEMTs application.

3.1.2. Effect of pressure and Ammonia flow on InAlN

Table III: $In_xAl_{1-x}N$ samples growth parameters summary along with their LayTec in-situ estimated thickness, RMS surface roughness, and Hall measurement data.

Sample	P (mbar)	$Q_{vol}NH_3$ (sccm)	Thickness (nm)	RMS roughness (nm)	μ_n (cm^2/Vs)	n_s ($x10^{12}$ cm^{-2})
1	70	1500	285.24	3.8	408	4.07
2	100	1500	279.74	4.3	176	3.0
3	150	1500	325.68	6.77	188	2.56
4	200	1500	320.02	8	31	0.14
5	70	2000	303.25	9.5	454	5.65
6	70	2500	301.91	7.97	360	4.96
7	70	3000	296.12	6	387	4.94
8	200	3000	270.87	10.5	43	0.011

Auger depth profile of sample 1, 4, 7 and 8 is shown in Figure 3.3 to qualitatively and relatively analyze the influence of pressure and NH_3 flow on In, Al, Ga, C and O. Ga auto incorporation due to its memory effect depend on growth conditions. For sample 1 this is negligible after the growth of 100 nm thick $In_xAl_yGa_{1-x-y}N$ layer. Nevertheless, when for the same pressure 70 mbar but with double NH_3 flow, sample 7 has relatively increased Ga incorporation but not significantly observed after the growth of 150 nm thick $In_xAl_yGa_{1-x-y}N$ layer. In Sample 4, $In_xAl_yGa_{1-x-y}N$ layer thickness is ~320 nm and do not have Ga incorporation in the top 100 nm layer and beyond that Ga is increasing linearly towards GaN buffer. This could be because of the higher pressure and larger thickness that all

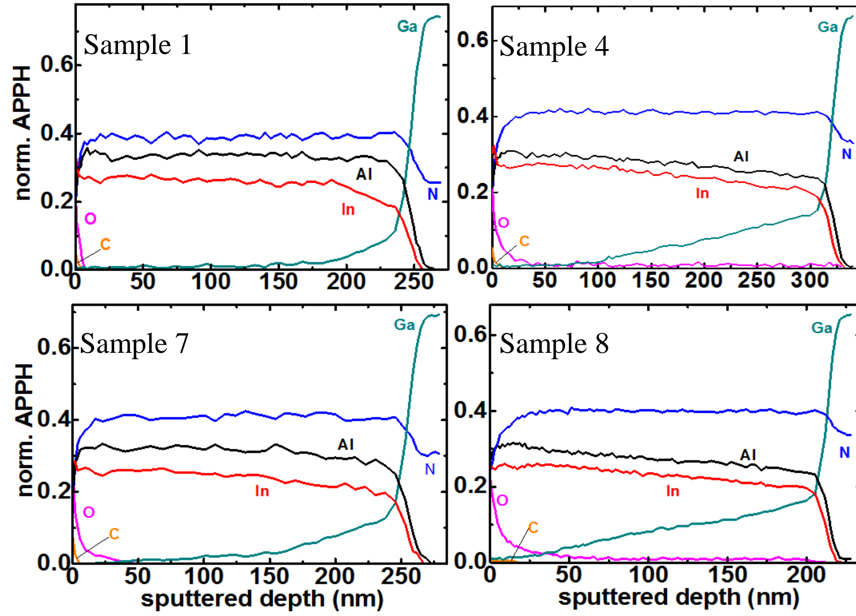

Figure 3.3. AES depth profile of sample 1- 70 mbar, sample 4- 200 mbar grown at NH_3 flow 1500 sccm, sample 7- 70 mbar and sample 8- 200 mbar at 3000 sccm NH_3 flow.

Ga remnant incorporated during early stage of growth. Sample 8 with double NH_3 flow than sample 4 have double available H_2 also which leads to the linearly decreasing Ga incorporation profile towards the surface and slightly alter the In incorporation.

At fixed NH_3 flow of 1500 sccm, In composition increased by 1% with increasing pressure from 70 to 200 mbar. However, at fixed pressure 70 mbar, In composition is not influenced by NH_3 flow of 1500 to 3000 sccm. Nevertheless, XRD results showed that $In_xAl_{1-x}N$ grown at 200 mbar and 3000 sccm NH_3 flow has 40.7 % In. Physical and chemical properties of $In_xAl_yGa_{1-x-y}N$ layers are influenced by pressure and NH_3 flow variation. AES, XPS and RBS data confirmed that, changes in pressure and NH_3 flow, alter the elemental depth profile within $In_xAl_yGa_{1-x-y}N$ layers. The quaternary compositional variation in $In_xAl_yGa_{1-x-y}N$ layers leads to the differences in the PL and absorption spectra. Higher pressure is favorable for reducing N vacancies. N vacancies could be further compensated by C and passivated by H at higher pressure that leads to decreased carrier concentration. Surface RMS roughness plays an important role while deciding the properties of a material.

3.1.3. Effect of strain on In-incorporation in InAlN layers

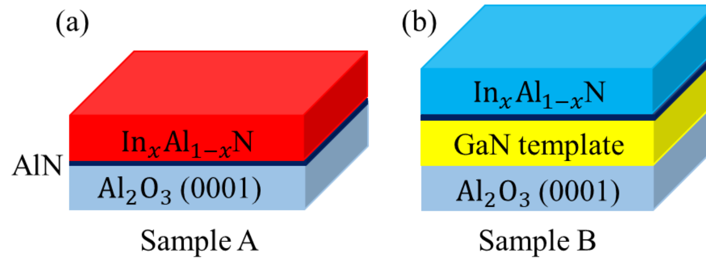

Figure 3.4. (a) Schematic layer structure illustration for sample A. The deposition was initiated with nitridation, followed by a 1-2 nm-thick HT-AlN nucleation layer and 334 nm-thick $In_xAl_{1-x}N$ layer. (b) Schematic layer structure illustration for sample B. The layer structure consists of a ~2μm-thick GaN template grown on Al_2O_3 (0001), and $In_xAl_{1-x}N$ layer.

The In-incorporation in $In_xAl_{1-x}N$ layer was approximately two times higher when grown on sapphire (In-molar fraction 0.60, sample A) compared to GaN template (In-molar fraction 0.28, sample B). Figure 3.5 shows a typical 2θ/ω XRD scan of sample A observed in broad range from 30.5 to 36.5°. The full width at half maximum (FWHM) of $In_{0.60}Al_{0.40}N$ 0002 peak observed at 33.07° in 2θ/ω scan is 0.20°. No diffraction peaks are observed at the positions expected for pure InN 0002 at 31.33° and for pure AlN 0002 at 36.14°, which indicates that the obtained 334 nm thick $In_{0.60}Al_{0.40}N$ layer has a single-phase structure and desired growth orientation.

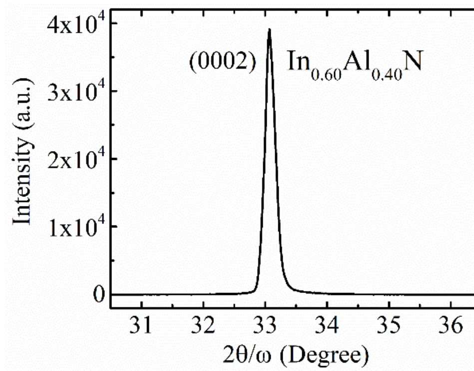

Figure 3.5. Representative XRD 2θ/ω scan of $In_{0.60}Al_{0.40}N$ grown on (0001) sapphire.

In order to track the In, N, Al, oxygen (O) and carbon (C) profiles of samples A and B along [0001] direction, AES depth profile was measured and the typical AES profiles are shown in Figure 3.6. Due to a mixing of atoms sputtered from very thin AlN layer with the atoms originating from adjacent layers at the high

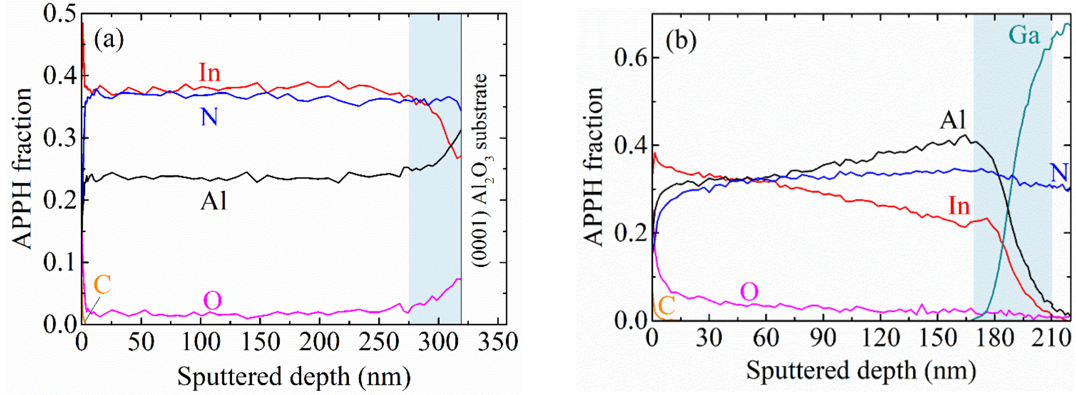

Figure 3.6. In, N, Al, O and C elemental depth profiles in $In_xAl_{1-x}N$ layers along the growth direction [0001] for (a) sample A and (b) sample B. Thickness of $In_xAl_{1-x}N$ layers of sample A and B is approximately 334 nm and 210 nm, respectively. The light blue area is corresponding to the transition region.

sputtering rates during AES depth profiling, the 1-2 nm thick AlN layer, as shown in Figure 3.4, is not visible in AES profiles of samples. Evidently, $In_xAl_{1-x}N$ layer of sample A consists of two different regions with different molar fractions: a transition region (light blue region) and a uniform region. In the transition region, In- and Al-molar fractions vary, while they remain nearly the same in the uniform region. For sample A, the Al-molar fraction falls and the complimentary In-molar fraction rises rapidly in the initial stage of growth, which corresponds to 50 nm thick transition region (at the depth ≥275 nm). With the progression of growth, the In-molar fraction enters into the uniform region with In-molar fraction of 0.60. In the case of sample B, $In_xAl_{1-x}N$ layer growth mechanism seems to be additionally complicated due to the existing Ga profile in the transition regions, which could be out-diffused from the underlying GaN layer.[9] We did not observe unwanted Ga in $In_xAl_{1-x}N$ layer of sample A that ruled out growth environment and lingering precursors for being the source of Ga in the transition region of sample B.[10]

The observed different thicknesses or growth rates of $In_xAl_{1-x}N$ layers of samples A (~0.04 nm/s) and B (~0.02 nm/s), indicate that not only In-incorporation, but also that the growth rate is influenced by different under-lying substrates. This indicate that In-incorporation efficiency depends on growth rate. Typically, the high defect density in a layer arise from the large residual in-plane strain that is generated by the large lattice mismatch to the used substrate and consequently, relaxed

$In_xAl_{1-x}N$ layer of sample A could provide a favorable accommodation to the larger size of In adatoms.

3.2. Growth and properties of InN/InAlN heterostructures

To grow InN on InAlN, several attempts have been tried and InN was successfully grown at 600 °C in sample D. Keeping all growth parameters same as of sample D, then we chose to increase TMIn flow. Increase of TMIn flow, which supplies proper In ad-atoms to the substrate and subsequently InN layer form. XRD 0002 scans of samples is shown in Figure 3.7. A significant improvement in single

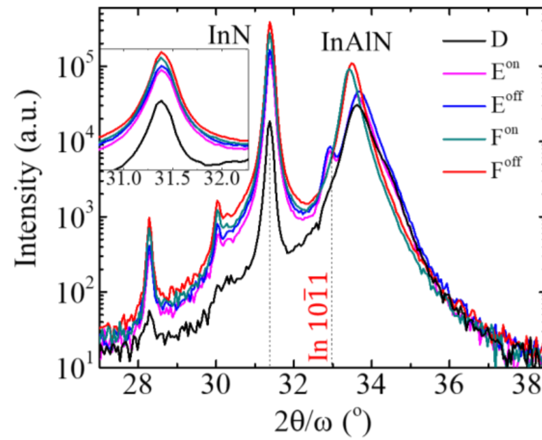

Figure 3.7. XRD 0002 2θ/ω scans of InN/InAlN HSs. Diffraction 0002 peaks of InAlN and InN are distinctly visible. Note the improved crystal quality of InN layers in inset. Peaks appeared at 28° and 30° are parasitic peaks.

crystal InN layer quality is observed with the three times increase in TMIn flow from 15 sccm to 45 sccm. Samples E^{off} and E^{on} also exhibit In $10\bar{1}1$ peak tough. The negative role of hydrogen in the occurrence of In become clear as we switched heater purge to nitrogen. Disappeared In $10\bar{1}1$ peak with a slight improve in InN quality in samples F^{off} and F^{on} is accompanied by a shift in InAlN peak as well. We believe, this shift in InAlN peak, which make it asymmetric, may be due to the changed property of the InN/InAlN interface in N-rich ambient.

Taking advantages of the steps created in vicinal surface of 4°off sapphire as a nucleation sites, high nucleation density and subsequently better coalesced InN layer is observed in sample F^{off} in comparison to F^{on}. In other words, this validates the epitaxial growth of InN layer in miscut sapphire substrates as well and grown layers

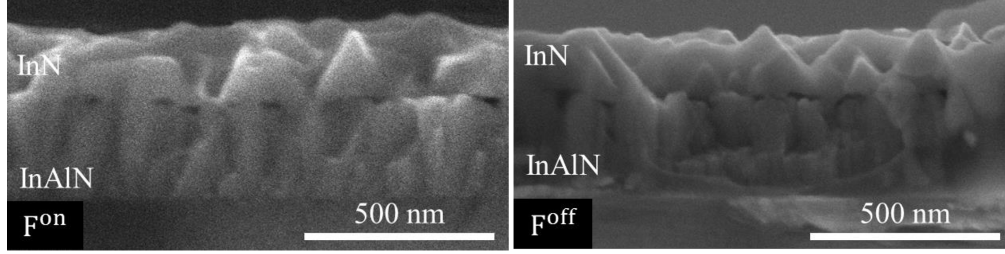

Figure 3.9. Cross-sectional SEM image of the interface between InN and InAlN of sample F grown on c-sapphire and 4°off sapphire. The height of voids between InN and InAlN is approximately 20 nm. Thickness of InAlN is ~260 nm and of InN ~150 nm.

follow the same lattice structure as of substrates. To investigate the charge transportation in quantum well (QW) formed in InN/InAlN HS, Hall measurement on samples was performed and summarized in Table IV. The discontinuity of the InN layers and presence of voids at the InN/InAlN interface (shown in Figure 3.9) could affect the Hall measurements. Improved layer homogeneity and interface properties of InN/InAlN HSs grown at 45 sccm TMIn and also on 4°off sapphire is also reflect in the Hall measurements. Furthermore, Hall electron mobility of samples F^{off} is more than sample E^{off}. This could be attributed to the surface and/or scattering mechanisms. For our still un-optimized InN/InAlN HSs, the observed highest Hall electron mobility in sample F^{off} is very encouraging for us.

Table IV. Electrical characteristics of InN/InAlN HSs.

TMIn flow rate (sccm)		Sheet carrier concentration cm^{-2}	Mobility cm^2/Vs
15		Isolated islands	-
30	E^{off}, 4°off sapphire	$1.6x10^{14}$	199
	E^{on}, c- sapphire	$2x10^{14}$	179
45	F^{off}, 4°off sapphire	$1x10^{14}$	469
	F^{on}, c- sapphire	$1.2x10^{14}$	396

With this we would conclude that the present work shows the successful growth of single crystalline InN, and to our knowledge, we prepared the first InN/InAlN HS ever. Nevertheless, further optimisation is needed to improve material quality and to grow device grade InN/InAlN heterostructure.

Summary

The first two chapters introduced the importance, challenges and key words of the research topic to the reader. The third chapter described the experimental work in two sections. In the first section growth of In-rich InAlN and in second section growth InN layers has been reported. High crystalline quality 334 nm thick InAlN layer with 0.60 In-molar fraction and smooth surface morphology was achieved directly on sapphire. To grow good quality single crystalline InN epitaxial layer on InAlN by OMCVD, InN growth temperature and TMIn flow have been studied on different substrates (c-plane and 4°off sapphire, free standing GaN) in this work. Last but not the least with the growth of InN channel layer on optimized In-rich InAlN buffer layer, in this dissertation thesis work we report the successful growth of III-N quantum structures for new generation of ultra-fast transistors.

List of publications

[ADC01] Dobročka, E., Hasenöhrl, S., **Chauhan**, P., and Kuzmík, J.
Non-conventional scans in high-resolution X-ray diffraction analysis of epitaxial systems,
Applied Surface Sci. 461 (2018) 23-32.

[ADC02] **Chauhan**, P., Hasenöhrl, S., Dobročka, E., Vančo, Ľ., Stoklas, R., Kováč, J., Šiffalovič, P., and Kuzmík J.
Effect of temperature and carrier gas on the properties of thick $In_xAl_{1-x}N$ *layer*,
Applied Surface Sci. 470 (2019) 1-7.

[ADC03] Hasenöhrl, S., **Chauhan**, P., Dobročka, E., Stoklas, R., Vančo, Ľ., Veselý, M., Bouazzaoui, F., Chauvat, M.-P., Reterana, P., and Kuzmík, J. *Generation of hole gas in non-inverted InAl(Ga)N/GaN heterostructures*, Applied Phys. Express 12 (2019) 014001.

[ADC04] **Chauhan**, P., Hasenöhrl, S., Dobročka, E., Chauvat, M.-P., Minj, A., Gucmann, F., Vančo, Ľ., Kováč, J.jr., Kret, S., Ruterana, P., Kuball, M., Šiffalovič, P., and Kuzmík, J.
Evidence of relationship between strain and In-incorporation: growth of N-polar In-rich InAlN buffer layer by OMCVD,
J. Applied Phys. 125 (2019) 105304.

[ADC05] **Chauhan**, P., Hasenöhrl, S., Minj, A., Chauvat, M.P., Ruterana, P., and Kuzmík, J.
Growth evolution of N-polar Indium-rich InAlN layer on c-sapphire via strain relaxation by ultrathin AlON interlayer,
Applied Surface Sci. (2019) (accepted).

[AFD01] **Chauhan**, P., Hasenöhrl, S., Dobročka, E., Stoklas, R., Czímerová, A., and Kuzmík, J.
Effect of growth temperature on the structural, optical and electrical properties of the InAlN/GaN heterostructure grown on C-sapphire by MOCVD,
In: 19th Conf. of Doctoral Students FEEIT STU. Bratislava, FEI STU 2017.

[AFD02] **Chauhan**, P., Hasenöhrl, S., Hulman, M., Kováč, J., Rosová, A., Šiffalovič, P., and Kuzmík, J.
Study of surface morphology and optical properties of InAlN epilayers grown on c-sapphire at different temperatures by MOCVD
In: 5st Int. Conf. on Advan. in Electronic and Photonic Technol. ISBN 978-80-554-1342-6. P. 125-128.

[AFD03] **Chauhan**, P., Hasenöhrl, S., Dobročka, E., Stoklas, R., Vančo, Ľ., Kováč, J. Jr., Machajdík, D., Kobzev, A. P., Šiffalovič, P., Kuzmík, J. *Growth of InAlN by MOCVD,*
In: Int. Workshop on devices and applications, OSIRIS workshop 2017, STU FEI, Bratislava, Slovakia.

[AFE01] Dobročka, E., Hasenöhrl, S., **Chauhan**, P., and Kuzmík, J.
Non-conventional scans in highresolution X-ray diffraction analysis of epitaxial systems,
In: 5th Int. Conf. "Progress in Applied Surface, Interface and Thin Film Science-Solar Renewable Energy News", Florence 2017.

[AFE02] Hasenöhrl, S., **Chauhan**, P., Dobročka, E., Stoklas, R., Vančo, Ľ., Vesely, M., Gucmann, F., Kuball, M., and Kuzmík, J.
Generation of Hole Gas in Non-inverted InAl(Ga)N/GaN Heterostructures,
In: Int. Workshop on Nitride Semicond. (IWN 2018) Kanazawa 2018.

[AFK01] Hasenöhrl, S., Gregušová, D., Dobročka, E., Stoklas, R., **Chauhan**, P., and Kuzmík, J.
MOCVD growth of GaN/AlGaN 2 DEG structures with InGaN cap for examination of polarization charge engineering concept in normally–off GaN MOS-HEMTs,
In: 17th European Workshop on Metal-Organic Vapour Phase Epitaxy (EW-MOVPE 17). Grenoble 2017.

[AFK02] Hasenöhrl, S., **Chauhan**, P., Dobročka, E., Stoklas, R., Vančo, Ľ., and Kuzmík, J.
Study of Indium incorporation in OMVPE grown 200-nm Thick $In_xAl_{1-x}N$ *layers*,
In: Int. Symp. on Growth of III-Nitrides - ISGN-7. Varšava 2018.

[AFK03] **Chauhan**, P., Hasenöhrl, S., Dobročka, E., Vančo, Ľ., Bouazzaoui, F., Gucmann, F., Chauvat, M.P., Kovac, J., Vesely, M., Ruterana, P., Kuball, M., and Kuzmík, J.
OMVPE growth of $InxA_{l1-x}N$ *layer on different substrates*,
In: Int. Workshop on Nitride Semicond. (IWN 2018) Kanazawa 2018.

References

[1] J. Kuzmík, “Proposal of normally-off InN-channel high-electron mobility transistors,” Semiconductor Science and Technology, vol. 29, no. 3, p. 035015, 2014.

[2] Michiel Vandemaele, “Numerical simulation of InN based HEMTs”, Master’s thesis, Department of Microtechnology and Nanoscience, Chalmers Univ. of Technol., Gothenburg, Sweden 2015.

[3] Brian E. Foutz et al., “Transient electron transport in wurtzite GaN, InN, and AlN,” Journal of Applied Physics 85, 7727 (1999).

[4] R. Quay, “Gallium nitride electronics,” vol. 96. Springer, 2008.

[5] Akinori Koukitu et al., “Thermodynamic Study on Metalorganic Vapor-Phase Epitaxial Growth of Group III Nitrides,” Jpn. J. Appl. Phys. 36, L1136-L1138, 1997.

[6] Akinori Koukitu and Hisashi Seki, “Unstable Region of Solid Composition in Ternary Nitride Alloys Grown by Metalorganic Vapor-Phase Epitaxy,” Jpn. J. Appl. Phys. 35 L1638-L1640, 1996.

[7] Suk Choi et al., “Origins of unintentional incorporation of gallium in InAlN layers during epitaxial growth, part I-effects of underlying layers and growth chamber conditions,” Journal of Crystal Growth 388, 137–142, (2014).

[8] J. Kuzmik, “InAlN/(In)GaN high electron mobility transistors: some aspects of the quantum well heterostructure proposal,” Semicond. Sci. Technol. 17 (2002) 540.

[9] J. J. Zhu et al., Contribution of GaN template to the unexpected Ga atoms incorporated into AlInN epilayers grown under an indium-very-rich condition by MOCVD, J. Cryst. Growth 348 (2012) 25.

[10] M. D. Smith, E. Taylor, T. C. Sadler, V. Z. Zubialevich, K. Lorenz, H. N. Li, J. O'Connell, E. Alves, J. D. Holmes, R. W. Martin and P. J. Parbrook, Determination of Ga auto-incorporation in nominal InAlN epilayers grown by MOCVD, J. Mater. Chem. C 2 (2014) 5787.